Behavior of underground strutted retaining structure under seismic condition

Subha Sankar Chowdhury[a], Kousik Deb[*] and Aniruddha Sengupta[b]

Department of Civil Engineering, Indian Institute of Technology Kharagpur, Kharagpur–721302, India

Abstract. In this paper, the behavior of underground strutted retaining structure under seismic condition in non-liquefiable dry cohesionless soil is analyzed numerically. The numerical model is validated against the published results obtained from a study on embedded cantilever retaining wall under seismic condition. The validated model is used to investigate the difference between the static and seismic response of the structure in terms of four design parameters, e.g., support member or strut force, wall moment, lateral wall deflection and ground surface displacement. It is found that among the different design parameters, the one which is mostly affected by the earthquake force is wall deflection and the least affected is the strut force. To get the best possible results under seismic condition, the embedment depth of the wall and thickness of the wall can be chosen as around 100% and 6% of the depth of final excavation level, respectively. The stiffness of the strut may also be chosen as 5×10^5 kN/m/m to achieve best possible performance under seismic condition.

Keywords: diaphragm wall; strutted excavation; FLAC; sand; earthquake

1. Introduction

The behavior of permanent underground retaining structures such as underground basement or metro station is usually studied under static condition only. However, if these are constructed in areas which are prone to earthquakes, then seismic forces may affect their behavior significantly. The effect of earthquake may become detrimental and cause collapse of the entire retaining system due to failure of wall and support system when excessive load and moment come in the struts and wall due to the dynamic earth pressure behind the retaining wall. Moreover, the ground surface adjacent to the retaining wall may also settle or heave beyond permissible limit under seismic condition creating severe instability of the adjacent structures.

A number of analyses on underground retaining structures have been done under static condition either using finite element methods (Finno and Harahap 1991, Finno *et al*. 1991, Day and Potts 1993, His and Small 1993, Bose and Som 1998, Ng *et al*. 1998, Carruba and Colonna 2000, Karlsrud and Andresen 2005, Zdravkovic *et al*. 2005, Costa *et al*. 2007, Yoo and Lee 2008, Hsiung 2009, Ou and

---

*Corresponding author, Ph.D., Associate Professor, E-mail: kousik@civil.iitkgp.ernet.in
[a]E-mail: chowdhurysubha@gmail.com
[b]Professor, E-mail: sengupta@civil.iitkgp.ernet.in

Hsieh 2011) or with the help of empirical or semi-empirical methods based on numerous databases on deep excavation from worldwide case histories in different types of soil (Hsieh and Ou 1998, Tanaka 1999, Long 2001, Moormann 2004, Liu *et al*. 2005, Wang *et al*. 2005, 2010, Kung *et al*. 2007). The static behavior of braced excavation has also been studied with physical model tests (Georgiadis and Anagnostopoulos 1999, Nakai *et al*. 1999, Takemura *et al*. 1999, Tefera *et al*. 2006). But very limited studies on such structures under seismic condition have been conducted.

Callisto and Soccodato (2010) have utilized acceleration time history of two Italian earthquakes to perform numerical analyses of embedded cantilever retaining walls in dry coarse-grained soil using FLAC. The behavior of the retaining walls has been studied by pseudo-static approach and a design criterion has been developed. Apart from the embedded retaining wall, a number of numerical studies (Neelakantan *et al*. 1992, Siller and Frawley 1992, Yogendrakumar *et al*. 1992, Madabhushi and Zeng 1998, 2008, Jr. Richards *et al*. 1999, Caltabiano *et al*. 2000, Gazetas *et al*. 2004, Ling *et al*. 2005, Psarropoulos *et al*. 2005, Wartman *et al*. 2006) have been done on other type of walls such as gravity, cantilever, anchored walls or mechanically stabilized earth retaining walls under seismic condition. Experimental studies (Zeng 1998, Tufenkjian and Vucetic 2000, Watanabe *et al*. 2003, Ling *et al*. 2005, 2009, Atik and Sitar 2010) have also been conducted to investigate the behavior of different types of wall under seismic condition. Conti *et al*. (2010) conducted dynamic centrifuge tests on scaled models of flexible retaining walls, both cantilevered and singly propped at the top. It was identified that the permanent displacements (during shaking) and residual bending moments (after shaking) depend not only on the entire acceleration time history, but also on current earthquake intensity. It is observed that most of the seismic studies have been conducted to investigate the behavior of cantilever or gravity wall retaining backfill soil (or sheet piles). Very limited studies have been conducted on embedded retaining structures under seismic condition because they are most of the time temporary in nature. In view of this, an attempt has been made in this paper to study the behavior of embedded retaining structures during earthquakes. In this study, the force in the supporting members (struts or slabs), bending moment in the wall, deflection of the wall and the vertical ground displacement under seismic condition have been compared with those under static condition to assess the effect of earthquake on the performance of embedded retaining structures.

2. Numerical simulation

Both static and seismic analyses have been done using a two dimensional plane strain finite difference program called FLAC (Itasca 2005). The construction of embedded retaining structure involves different stages of excavation and subsequent installation of support members at the desired levels below the ground until final excavation level is reached. In the numerical computation, the characteristic of the soil under dynamic condition is described by a hysteretic model which updates the tangent shear modulus at each calculation step. The soil behaves as a linearly elastic-perfectly plastic material following Mohr-Coulomb failure criterion.

The schematic diagram of an underground permanent retaining structure with diaphragm wall and supports and the problem geometry considered in the present study is shown in Fig. 1. The specific geometry which has been chosen in the present analysis is a typical system taken from Chowdhury *et al*. (2013) for analysis under static condition. The values of the excavation depth, embedment depth of wall, wall thickness and the position of the struts below ground level as shown in Fig. 1 are within the range of their optimum values as mentioned in Chowdhury *et al*.
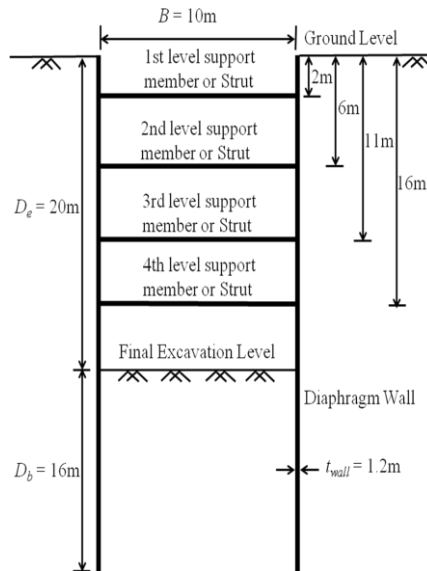
Fig. 1 Schematic diagram of geometry considered in the present study

(2013). In case of an underground structure such as a station building for underground metro transport, the R.C.C diaphragm walls becomes permanent and these walls are connected with slabs at different levels. These slabs are the support members which run throughout the length of the wall. In the present analysis, the walls and the struts are modeled so to simulate diaphragm wall and the slabs, respectively.

As different stages are involved in the construction of a braced excavation, theoretically earthquake may occur at any stage. However, the maximum chance of earthquake occurrence is at the service stage, i.e., at the final stage of construction. In the present study, each stage of the construction is first analyzed under static condition with small strain shear modulus ($0.3G_0$) and then under seismic condition with G_0. The stiffness (shear modulus, G_0) of soil changes with the strain level, but the model which has been used in the present study does not consider the reduction of stiffness with strain level. Thus, to incorporate the stiffness reduction, a reduced stiffness has been used during each stage analyzed under static condition as suggested by Aversa *et al*. (2007).This procedure is followed for all the stages till the final excavation level is reached. The values of the design parameters like bending moment, strut forces, wall deflection may reach maximum at any stage of the construction. However, the maximum ground deformation has been found to occur at the final stage of construction. As the ratio of the length to width of the excavation is usually very large, so it is analyzed as a two-dimensional plane strain problem. Considering unit length along the direction perpendicular to the plane of analysis, cross-sectional area (A_{wall}) and moment of inertia (I_{wall}) of the wall are calculated as $1.0 \times t_{wall}$ and $1.0 \times t_{wall}^3/12$ respectively, where t_{wall} is the thickness of the wall. Depending on the depth of excavation (D_e), the wall is supported by different levels of supporting members or struts. For 10 m, 15 m and 20 m depths of excavation, the number of strut is assumed to be 2, 3 and 4, respectively. The soil properties namely, dry density, friction angle and initial shear modulus are taken from Callisto and Soccodato (2010). The wall is embedded in dry, coarse-grained soil with a friction angle (ϕ) of 35° and density (ρ) of 2040 kg/m^3. The coefficient of lateral earth pressure at rest (K_0) is calculated

from (1-sinϕ). The initial stress state is computed by assuming K_0 as 0.426 (for ϕ equal to 35°). The sand layer is underlain by rigid layer at the bottom of the model. The wall friction angle (δ) between soil and wall is taken as 20°. A non-associated flow rule is used with dilatancy angle equal to zero. The Poisson's ratio (μ) of soil is taken as 0.30. The small strain shear modulus (G_0) varies with the mean effective stress (p') according to the following equation (Itasca 2005)

$$\frac{G_0}{p_{ref}} = K_G \left(\frac{p'}{p_{ref}} \right)^{0.5}$$
(1)

where, p_{ref} is the reference pressure (100 kPa), p' is the mean effective stress and K_G is the stiffness multiplier (equal to 1000). The values of p_{ref} and K_G are taken from Callisto and Soccodato (2010).

The first stage of the numerical analysis consists of installation of the wall in the soil under at rest (K_0) state of stress. In this stage, the stress dependent dynamic stiffness is characterized by the shear stiffness of the soil which follows the empirical power law (Eq. (1)). After the initial stage i.e., when the wall is installed in the ground, the reduced value of the shear modulus ($0.3G_0$) is used for static simulation of the excavation. This is done because the model does not allow the change in soil stiffness with the strain level in static simulation (Aversa *et al.* 2007). After the static analysis, the shear modulus (G_0) is used for dynamic analysis. The bulk modulus for static analysis (K_{st}) and dynamic analysis (K_d) are given by Eqs. (2a) and (2b), respectively.

$$K_{st} = \frac{2(0.3G_0)(1+\mu)}{3(1-2\mu)}$$
(2a)

$$K_d = \frac{2G_0(1+\mu)}{3(1-2\mu)}$$
(2b)

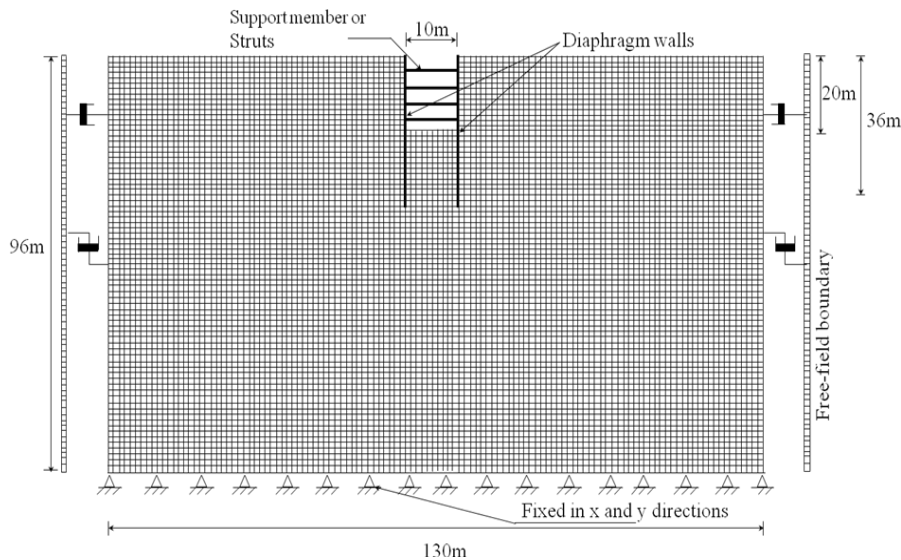The numerical model under seismic condition for 10m width of the excavation and 20m depth

Fig. 2 Numerical modeling for parametric study in FLAC

of excavation is shown in Fig. 2. In the model, the size of the elements is taken as 0.5 m$\times$0.5 m. The maximum frequency that can be modeled for smooth wave propagation through all elements depends on the minimum value of G_0 which is obtained at the centre of the topmost element of the model i.e., at a depth of 0.5/2=0.25 m below ground level. For ρ=2040 kg/m^3, p_{ref}=100 kPa and K_G=1000, the value of G_0 is found to be 1.8×10^7 kPa (as per Eq. (1)). The shear wave speed (C_s) and the maximum frequency (f_{max}) that can be modeled are calculated from the following equations (Itasca 2005) as

$$C_S = \sqrt{\frac{G_0}{\rho}} \tag{3}$$

$$f_{max} = \frac{C_S}{\lambda} \tag{4}$$

The value of C_s is 93.9 m/s. λ is the wavelength associated with highest frequency component that contains appreciable energy. The wavelength is calculated according to FLAC, 5.0 manual (Itasca 2005) as

$$\lambda = 10\Delta l \tag{5}$$

where Δl is the spatial element size i.e., 0.5 m. From Eqs. (3) and (4), the value of f_{max} is 18.6 Hz i.e., the maximum frequency with which the wave can propagate through the model is 18.6 Hz. So, the input acceleration history is low-pass filtered at 15 Hz for compatibility with the size of the elements. For all the chosen earthquakes, the majority of the power of the seismic wave is contained within the 15 Hz frequency as shown in Fourier spectra. So, by filtering the acceleration time history data at 15 Hz, there is no major loss of energy of the earthquake. Thus, the nature of the seismic motions remains similar, even after it is filtered at 15 Hz frequency.

During static simulation of the construction stages, the lateral boundaries are restrained from moving in horizontal direction and the bottom boundary is restrained from moving in both horizontal and vertical directions. During seismic analyses, free-field conditions are applied along the vertical boundaries so that boundaries retain their non-reflecting properties when these are subjected to outward propagating waves from the structure. The lateral boundaries of the main grid are connected with the free field grid by viscous dashpots to simulate quiet boundary condition as developed by Lysmer and Kuhlemeyer (1969).

The two vertical boundaries at the right and left edges of the model are kept at a distance of $6B$ (where, B is the width of excavation) from the left and right walls, respectively. Similarly, the bottom boundary is located at the same distance from the toe of the wall.

The interface normal and shear stiffness (K_n and K_s) are estimated according to the following equation (Itasca 2005) as

$$K_n = K_s = 10\max\left[\frac{\left(K+\frac{4}{3}G\right)}{\Delta z_{min}}\right] \tag{6}$$

where K and G are the bulk and shear moduli of the soil and Δz_{min} is the smallest width of an adjoining element in the normal direction to the interface. The maximum value of the above expression for all the elements adjoining the interface is considered in the calculation of interface

normal and shear stiffness.

In the numerical model, the element size adjacent to the wall is taken as 0.5 m. As small strain shear modulus (G_0) increases with depth below the ground surface, the maximum value of G_0 for 18m depth of the wall is obtained at the at the toe of the wall i.e., at a depth of 17.75 m below ground surface because in FLAC, the shear modulus is estimated at the centroid of each element. The value of G (in Eq. (6)) is equal to G_0 (obtained from Eq. (1) corresponding to p' at 17.75 m below ground level with ρ=2040 kg/m^3). The value of K (in Eq. (6)) is equal to K_0 (obtained from Eq. (2b) corresponding to the value of G_0 as mentioned above). The interface normal and shear stiffness are calculated using the value of K, G and Δz_{min} (=0.5 m) in the Eq. (6). For 18 m depth of retaining wall, the values of K and G are 4.55×10^8 kN/m^2 and 2.10×10^8 kN/m^2, respectively. With Δz_{min}=0.5 m, the values of K_n and K_s are 1.47×10^{10} kN/m^2. The cohesion and friction angle of the interface material are 0 and 20°, respectively.

The Young's modulus of the wall (E_{wall}) and Poisson's ratio of concrete (μ_{wall}) are taken as 29580 MPa and 0.15, respectively. In FLAC, the Young's modulus of the wall is given as $E_{wall}/(1-\mu_{wall}^2)$ in order to represent plane strain formulation of a continuous wall as mentioned in the FLAC (Itasca 2005). The walls and the struts are modeled using beam elements. If the cross-sectional area, modulus of elasticity and the spacing of support member are A_{strut}, E_{strut} and s, respectively, then the strut or support stiffness (k_{strut}) is given by $A_{strut}.E_{strut}/ls$, where l is the length of support member i.e., width of excavation. In the seismic analyses, the whole braced excavation is modeled with two walls situated at the two edges of the excavation and connected by supporting members or struts at different levels. The distance between the two walls is equal to the width of the excavation. The connection between the strut nodes and the wall nodes are established with the help of springs. Only rotation is allowed for the strut node i.e., hinge connection exists between the wall node and the strut node. The translation in both vertical and horizontal directions is not allowed for the strut node.

The soil behavior under the earthquake loading is described by non-linear model with hysteretic damping available in FLAC (Itasca 2005). Under plane strain condition, the shear stress (τ) and the shear strain (γ) are related as

$$\frac{\tau}{G_0} = \frac{G_s(\gamma)}{G_0}\gamma = M_s(\gamma).\gamma \qquad (7)$$

where $G_s(\gamma)$ is the secant shear modulus which is a function of γ, G_0 is the small strain shear modulus and M_s is the normalized secant shear modulus. In the present analysis, it is assumed that cyclic soil behavior can be represented by the relationship between M_s and γ given in FLAC (Itasca 2005). The modulus degradation curve is expressed using the sigmoidal model in FLAC (Itasca 2005) and is given by

$$M_s = y_0 + \frac{a}{1+exp\left[-\left(log_{10}\gamma - x_0\right)/b\right]} \qquad (8)$$

where the values of the four parameters are given by a=0.9762, b=-0.4393, x_0=-1.285 and y_0=0.03154.

The details of the three chosen earthquakes, i.e., Loma Prieta, Tolmezzo, and Northridge earthquakes, used in the present study are given in Table 1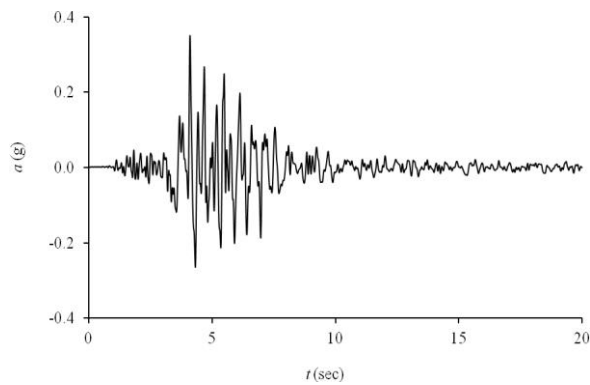. The input acceleration time history of Loma Prieta, Tolmezzo and Northridge earthquakes are shown in Figs. 3(a), (b), (c), respectively. In the figures, the input acceleration is given in the units of acceleration due to

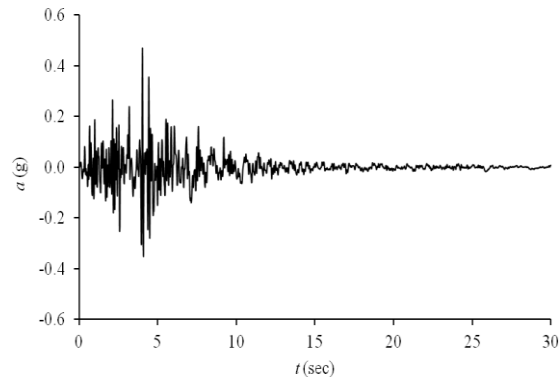Table 1 Earthquakes considered in the present study

Name of Earthquake	Year of occurrence	Duration (sec)	Peak ground acceleration (PGA) (g)
Loma Prieta	1989	40	0.28
Tolmezzo	1976	20	0.35
Northridge	1994	32	0.54
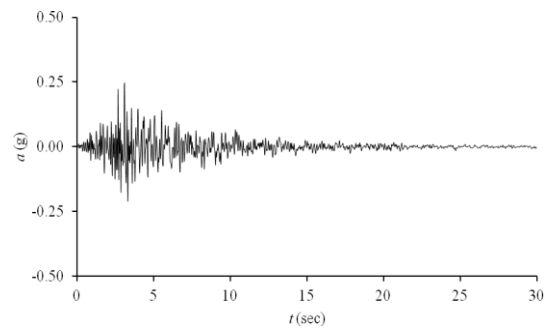
(a)

(b)

(c)

Fig. 3 Input acceleration time history for (a) Loma Prieta earthquake (b) Tolmezzo earthquake and (c) Northridge earthquake
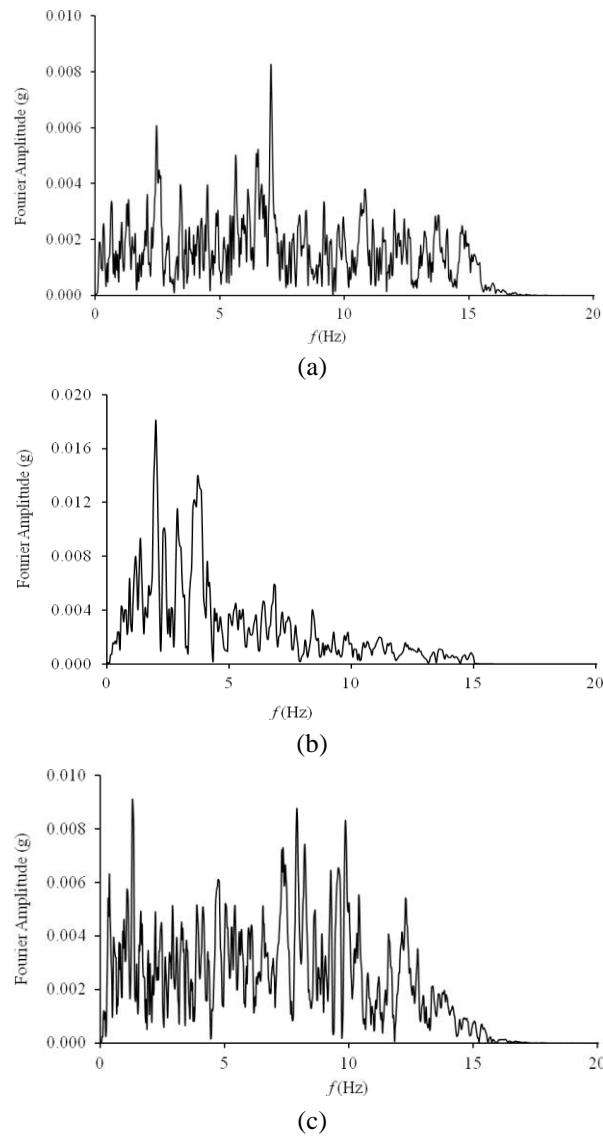
Fig. 4 Fourier amplitude spectrum of input acceleration history for (a) Loma Prieta earthquake (b) Tolmezzo earthquake and (c) Northridge earthquake

gravity (g) and time (t) in seconds. The frequency content of the earthquakes is determined by Fourier amplitude spectrum and it is shown in Figs. 4(a), (b), (c) for Loma Prieta, Tolmezzo and Northridge earthquakes, respectively. Each of the acceleration time histories is filtered at 15 Hz and is applied to the bedrock nodes at the bottom boundary of the model. The elastic response spectra for zero percent damping are shown in Figs. 5(a), (b), (c) for Loma Prieta, Tolmezzo and Northridge earthquakes, respectively. From the response spectra of the three earthquakes, it is revealed that they cover the period (or frequency) range wide enough for the concerned structure. The range of PGA is in between 0.28 g and 0.54 g. This range is wide and high enough to cover most of the known earthquakes.
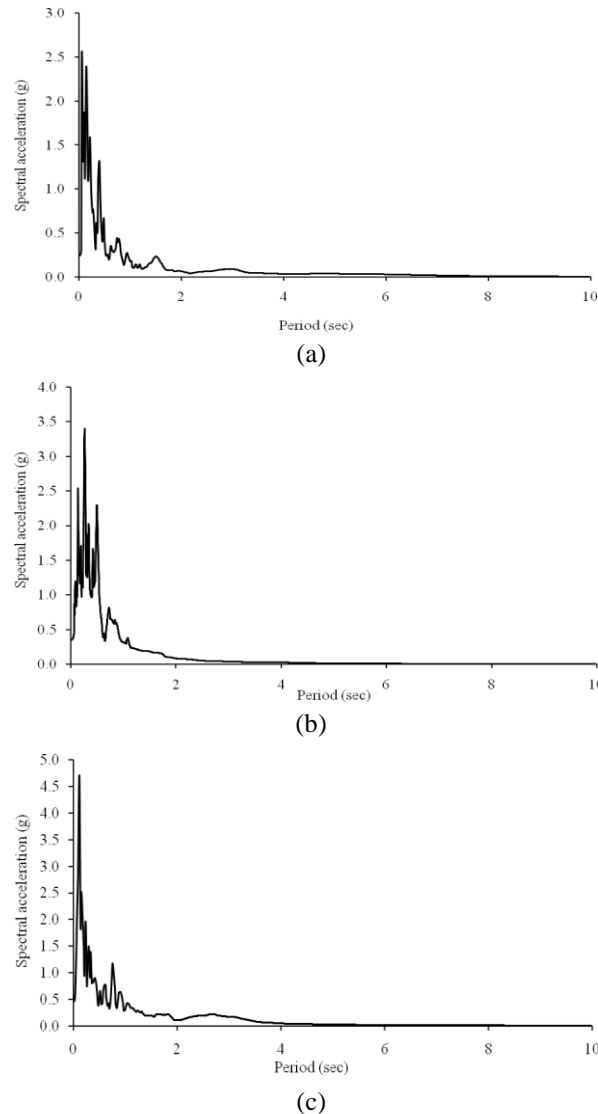
(a)

(b)

(c)

Fig. 5 Response spectrum of input acceleration history for (a) Loma Prieta earthquake (b) Tolmezzo earthquake and (c) Northridge earthquake

3. Results and discussions

3.1. Model validation

To validate the developed numerical model, two embedded cantilevered retaining walls, as presented by Callisto and Soccodato (2010), are modeled in FLAC. The retaining walls are made up of contiguous bored reinforced 0.6 m diameter concrete piles at 0.7 m spacing with a bending stiffness of 2.7×10^5 kN-m/m. The width of the excavation is 16 m. All the material properties and geometry are taken as reported in Callisto and Soccodato (2010). In the numerical model, the
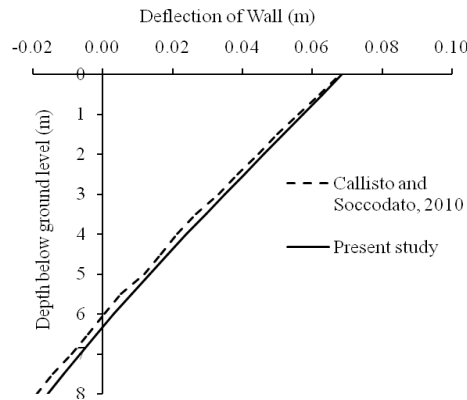
Fig. 6 A comparison between deflection patterns of left wall from Callisto and Soccodato (2010) and present study
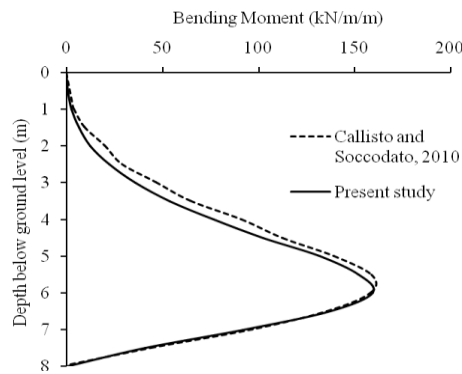

Fig. 7 A comparison between bending moment patterns in left wall from Callisto and Soccodato (2010) and present study

vertical boundaries extend upto 22 m from the edge of the wall and the horizontal boundary is also 22 m below the toe of the wall. The properties of the coarse-grained soil i.e., density (2040 kg/m^3), friction angle (35°), dilatancy angle (0°) and shear modulus (depends on mean effective stress, as per Eq. (1)) are taken from Callisto and Soccodato (2010). In the validation model, a small value of cohesion (=0.5 kN/m^2) of the soil is taken to ensure numerical stability (Callisto *et al.* 2008). The values of K_0 and μ for the soil are taken as 0.5 and 0.2, respectively. The deflection of the left wall and bending moment developed in the left wall at the end of the Tolmezzo earthquake are estimated in the present numerical study and the results are compared with the results obtained by Callisto and Soccodato (2010).

The deflection pattern of the left wall at the end of the earthquake as found from the present study and that from Callisto and Soccodato (2010) is presented in Fig. 6. It can be seen from the figure that the deflections predicted by the present study matches closely with that from Callisto and Socodato. However, the difference between the results increases as the depth of the wall increases. The variation of bending moment developed in the left wall with depth below ground level at the end of the earthquake found from the present study and Callisto and Soccodato (2010) is shown in Fig. 7. It may be observed from the figure that there is little difference between the

bending moment values upto 6 m depth below ground level. Below 6 m depth, the results match very closely. The small variation of the results obtained from the present study and Callisto and Soccodato (2010) may be due to the selection of different mesh size and time step.

3.2 Parametric study

A parametric study is done using the developed numerical model to investigate the effect of earthquake on the four design parameters i.e., maximum strut force (*F*), maximum wall moment (*M*), maximum wall deflection (*u*) and maximum ground surface displacement (*v*). A comparison has been made between the values of the four design parameters under static condition, at an instant during earthquake when maximum value is reached and at the end of the earthquake. The analyses are done for 10 m, 15 m and 20 m depths of excavation (D_e). The width of excavation is taken as 10 m. For each depth of excavation, analyses have been performed for three different earthquakes i.e., Loma Prieta (PGA=0.28 g) earthquake, Tolmezzo (PGA=0.35 g) earthquake, and Northridge (PGA=0.54 g) earthquake. Among the three earthquakes chosen for the analysis, Tolmezzo earthquake has been taken from Callisto and Soccodato (2010). Two other earthquakes are of different nature than Tolmezzo earthquake and they have been selected on the basis of the PGA values and nature of acceleration time history, so that the response of embedded retaining structure under seismic condition with different PGA may also be studied. The acceleration time histories of each earthquake are applied at the base of the model and the analysis is done for the whole duration of each earthquake, that is, 20s, 30s and 30s for Tolmezzo, Loma Prieta and Northridge earthquakes, respectively. The position of the struts below the ground level is shown in Table 2. The embedded depth (D_b), wall thickness (t_{wall}) and the strut stiffness are taken as 80% of D_e, 6% of D_e and 5×10^5 kN/m/m, respectively, which are as per recommendations given in Chowdhury *et al.* (2013) for static condition. Under static condition it is observed that the best possible result may be obtained (Chowdhury *et al.* 2013) if the type of strut arrangement is chosen as per Table 2, embedded depth of wall is between 80% to 100% of the depth of final excavation level (D_e), the thickness of the wall is 6% to 7% of the depth of final excavation level and stiffness of the strut or supporting member is between 5×10^5 kN/m/m to 25×10^5 kN/m/m. For initial parametric study, the values of the design parameters are chosen as per the recommendation given for static condition. To investigate the effect of strut stiffness, wall thickness and the embedment depth of the wall on the design parameters, three different analyses were done by considering strut stiffness equal to 25×10^5 kN/m/m, wall thickness as 7% of D_e i.e., 700 mm and embedment depth as 100% and 120% of D_e i.e., 10 m and 12 m. The values of embedment depths considered in the numerical analysis is similar to those in some of the case studies of deep excavation in sand or silty sand/ silty clay type of soil (Hsiung 2009, Kung 2009). In all these analyses, the values of the all other parameters are as per Chowdhury *et al.* (2013).

Table 2 Width, depth of excavation and support member (strut) arrangement considered in the parametric study

Width of excavation, *B* (m)	Depth of excavation, D_e (m)	Depth of struts below ground level (m)			
		1st strut	2nd strut	3rd strut	4th strut
10	10	2	6	-	-
	15	2	6	11	-
	20	2	6	11	16

3.2.1 Effect of earthquake on maximum strut force

A comparison between maximum strut force at different levels for different depths of excavation under static and seismic conditions is shown in Table 3. The strut forces under static condition (F_{stat}), at the end of earthquake and its maximum value at a particular instant during earthquake (F_{seis}) are shown for all the three earthquakes considered in the present study. If R_F is defined as the ratio of F_{seis} and F_{stat}, then it is found that when depth of excavation is 15 m, the

Table 3 Variation of Strut forces for different values of D_e and earthquakes

D_e (m)	Strut levels	Static (F_{stat})	Strut force ($\times 10^3$ kN/m)								
			Earthquake								
			Loma Prieta (PGA=0.28 g)			Tolmezzo (PGA=0.35 g)			Northridge (PGA=0.54 g)		
			End of EQ.	Maximum (F_{seis})	F_{seis}/F_{stat}	End of EQ.	Maximum (F_{seis})	F_{seis}/F_{stat}	End of EQ.	Maximum (F_{seis})	F_{seis}/F_{stat}
10	1st	0.74	1.78	1.97	2.66	1.97	2.38	3.21	2.03	2.16	2.92
	2nd	1.46	3.17	3.27	2.24	4.34	4.72	3.23	3.65	4.01	2.75
15	1st	0.87	1.83	1.97	2.26	1.95	2.44	2.80	1.86	2.34	2.69
	2nd	2.56	7.16	7.22	2.82	5.87	6.34	2.48	5.0	5.6	2.19
	3rd	2.50	3.08	5.19	2.08	6.74	6.95	2.78	6.84	6.84	2.74
20	1st	1.13	1.85	2.05	1.81	2.14	2.61	2.31	2.14	2.34	2.07
	2nd	2.92	4.8	5.06	1.73	7.41	7.56	2.59	5.77	6.16	2.11
	3rd	4.10	7.07	7.16	1.75	9.00	9.44	2.30	7.84	8.35	2.04
	4th	3.39	6.67	6.75	1.99	8.72	9.10	2.68	7.67	8.07	2.38

Table 4 Values of design factors for different values of D_b/D_e, t_{wall}/D_e and k_{strut} under static & seismic conditions

Design parameters		Values of design parameters									
		D_b=8 m, D_b/D_e=0.8 k_{strut}=5×10⁵ kN/m/m t_{wall}/D_e=0.06		D_b=10 m, D_b/D_e=1.0 k_{strut}=5×10⁵ kN/m/m t_{wall}/D_e=0.06		D_b=12 m D_b/D_e=1.2 k_{strut}=5×10⁵ kN/m/m t_{wall}/D_e=0.06		D_b=8 m D_b/D_e=0.8 k_{strut}=25×10⁵ kN/m/m t_{wall}/D_e=0.06		D_b=8 m D_b/D_e=0.8 k_{strut}=5×10⁵ kN/m/m t_{wall}/D_e=0.07	
		Static	Seismic (Max.)	Static	Seismic (Max.)	Static	Seismic (Max.)	Static	Seismic (Max.)	Static	Seismic (Max.)
F ($\times 10^3$ kN/m)	1st strut	0.737	2.379	1.136	3.317	2.33	4.775	0.852	2.531	0.745	2.152
	2nd strut	1.456	4.717	1.577	3.530	1.232	1.916	1.666	5.295	1.498	4.861
M ($\times 10^3$ kN-m/m)	Left	0.072	0.405	0.062	0.312	0.183	0.643	0.070	0.396	0.085	0.492
	Right	0.072	0.413	0.061	0.316	0.185	0.659	0.070	0.448	0.085	0.476
u (mm)	Left	1.51	79.32	1.376	78.3	4.50	75.96	1.424	80.33	1.407	79.95
	Right	1.51	84.38	1.356	84.32	4.60	90.56	1.428	84.44	1.398	83.37
v (mm)	Left	2.06	17.52	2.356	10.82	2.07	12.85	1.752	21.15	2.285	15.29
	Right	2.07	19.33	2.370	8.49	2.07	12.96	1.758	23.99	2.267	18.16

value of R_F for 1st, 2nd and 3rd levels varies from (2.3-2.8), (2.2-2.8) and (2.1-2.8), respectively for the selected earthquakes. Similarly, the value of R_F for 4th level strut, when D_e is 20 m, varies from 2.0 to 2.7. Thus, the maximum strut forces at a particular instant during an earthquake are approximately 2-3 times higher than that under static condition. However, the strut forces at the end of earthquake are approximately 1.2-3 times higher than that under static condition.

In order to investigate the effect of embedment depth, wall thickness and strut stiffness on axial force in struts under seismic condition, three different analyses were done and results are shown in Table 4. It can be found from Table 4 that, if the depth of embedment is increased from 8 m to 10 m the forces in 1st and 2nd level struts increase by 39% and decrease by 25%, respectively. However, if D_b is increased from 10 m to 12 m there is 44% increment and 46% decrement in 1st and 2nd level strut force, respectively. Similarly, for a particular value of D_b (=8 m) and t_{wall}/D_e (=0.06), if the strut stiffness (k_{strtu}) is increased from 5×10^5 kN/m/m to 25×10^5 kN/m/m, the forces in 1st and 2nd level struts increase by 6% and 12%, respectively. This is due to the fact that as the stiffness of the strut is increased, it attracts more force. However, when D_b=8 m, k_{strut}=5×10^5 kN/m/m and t_{wall}/D_e is increased from 0.06 to 0.07, the forces in 1st and 2nd level struts decreases by 10% and increases by 3%, respectively. Overall, it is observed that under seismic condition if the depth of embedment of the wall is taken as 100% of the depth of excavation, the best possible results can be obtained in terms of maximum strut force. However, maximum strut force increases as the stiffness of the strut and thickness of the wall increase.

3.2.2 Effect of earthquake on maximum wall moment

The value of the bending moment (M) has been estimated for both left and right walls under under static condition, at the end of earthquake and at a particular instant during earthquake when it is maximum. The distribution of the moment on the right wall along its depth is plotted in Figs. 8(a)-8(c), 9(a)-9(c), 10(a)-10(c) for three different depths of excavation and three different earthquakes. From the figures, it may be found that the moment under seismic condition is much greater than that under static condition. If the ratio between maximum bending moment at a particular instant during earthquake i.e., seismic moment (M_{seis}) and static moment (M_{stat}) is defined as R_M, then it is found that when D_e=10 m, 15 m and 20 m, the values of R_M are (6.2, 3.5 and 1.9), (5.7, 4.0 and 3.4) and (8.8, 3.2 and 2.8) for Loma Prieta, Tolmezzo and Northridge earthquakes, respectively. Thus, the maximum wall moment at a particular instant of earthquake is approximately 2-9 times higher than that under static condition. However, the wall moment at the end of earthquake is approximately 2-5 times higher than that under static condition.

It can be further found from Table 4 that if the depth of embedment is increased from 8m to 10m, the maximum seismic moment in the wall decreases by 23%. However, if D_b is increased from 10 m to 12 m there is 59% increment in the wall moment. Similarly, for a particular value of D_b (=8 m) and t_{wall}/D_e (=0.06), if the strut stiffness (k_{strut}) is increased from 5×10^5 kN/m/m to 25×10^5 kN/m/m, the maximum wall moment is increased by 8.5%. However, for D_b=8 m, k_{strut}=5×10^5 kN/m/m and t_{wall}/D_e is increased from 0.06 to 0.07, the maximum wall moment increases by approximately 20%. Thus, under seismic condition, if the depth of embedment of the wall is taken as 100% of depth of excavation, the best possible result can be obtained in terms of maximum wall moment. However, maximum wall moment increases as the stiffness of the strut and thickness of the wall increase.

3.2.3 Effect of earthquake on maximum lateral wall deflection

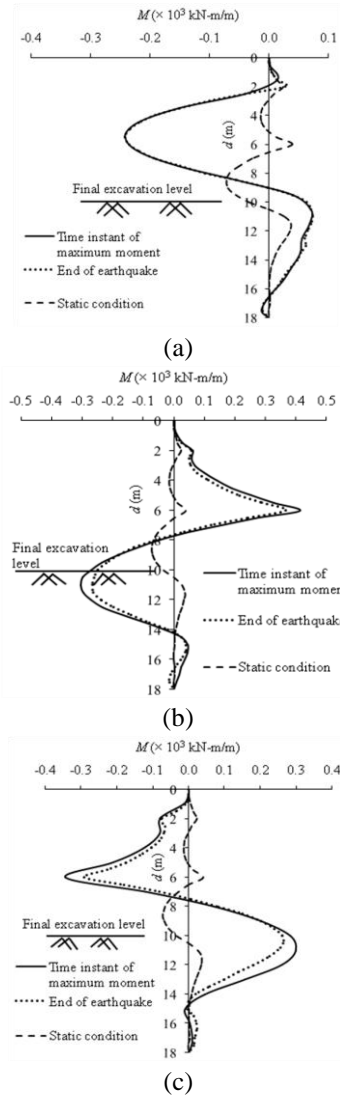The lateral wall deflection under static condition, at the end of earthquake and at the instant of

Fig. 8 Bending moment profile of right wall when D_e=10 m for (a) Loma Prieta earthquake (b) Tolmezzo earthquake and (c) Northridge earthquake

maximum value are shown in Figs. 11(a)-11(c), 12(a)-12(c), 13(a)-13(c) for three different depths of excavation and three different earthquakes. From the figures, it is seen that there is a large difference between the deflection under static and seismic conditions. If the ratio between the maximum value of the wall deflection under seismic condition (u_{seis}) and static condition (u_{stat}) is defined as R_u, then it is found when D_e=10 m, the values of R_u are 55.9, 51.4 and 87.1 for Loma Prieta, Tolmezzo and Northridge earthquakes, respectively. However, if D_e is 15 m, the values of R_u are 37.5, 35.2 and 61.0 for the selected earthquakes. Similarly, when the depth of excavation is 20 m, the values of R_u are 26.7, 29.1 and 45.1 for Loma Prieta, Tolmezzo and Northridge earthquakes, respectively. Thus, the maximum wall defection at a particular instant during earthquake is approximately 25-90 times higher than that under static condition. However, the wall

defection at the end of earthquake is approximately 7-58 times higher than that under static condition. For the selected soil profile, earthquake and structure, the ratio of seismic and static deflection (up to 90 at a particular instant during earthquake and 58 at the end of earthquake) may
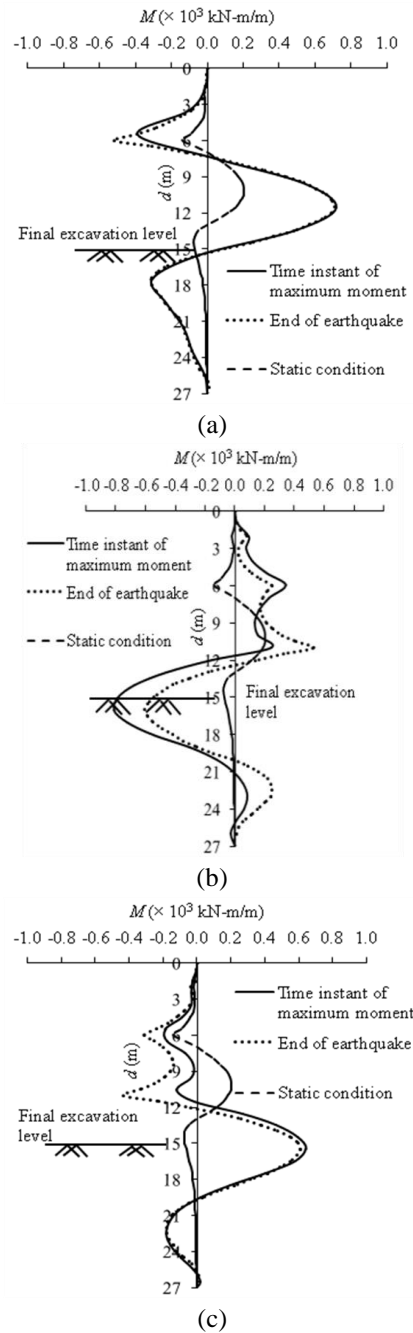

(a)

(b)

(c)

Fig. 9 Bending moment profile of right wall when D_e=15 m for (a) Loma Prieta earthquake (b) Tolmezzo earthquake and (c) Northridge earthquake
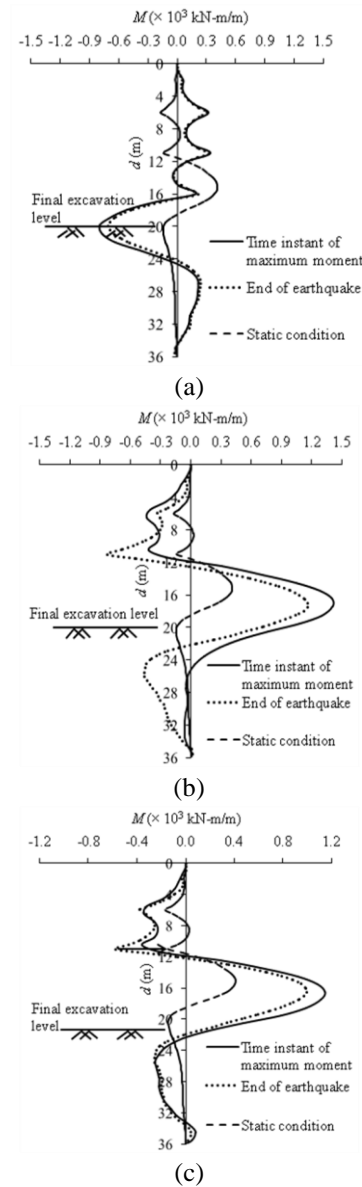
Fig. 10 Bending moment profile of right wall when D_e=20 m for (a) Loma Prieta earthquake (b) Tolmezzo earthquake and (c) Northridge earthquake

increases or decreases depending on the factors mentioned above. The seismic motions increase the earth pressure on underground structures. It also may have a kinematic effect on the underground structure (Abuhajar *et al.* 2011).

It is also found from Table 4 that if the depth of embedment is increased from 8 m to 10 m, the value of lateral wall deflection under seismic condition remains almost constant. However, if D_b is increased from 10 m to 12 m, there is 7% increment in the wall deflection. For a particular value of D_b (=8 m) and t_{wall}/D_e (=0.06), if the strut stiffness (k_{strut}) is increased from 5×10^5 kN/m/m to
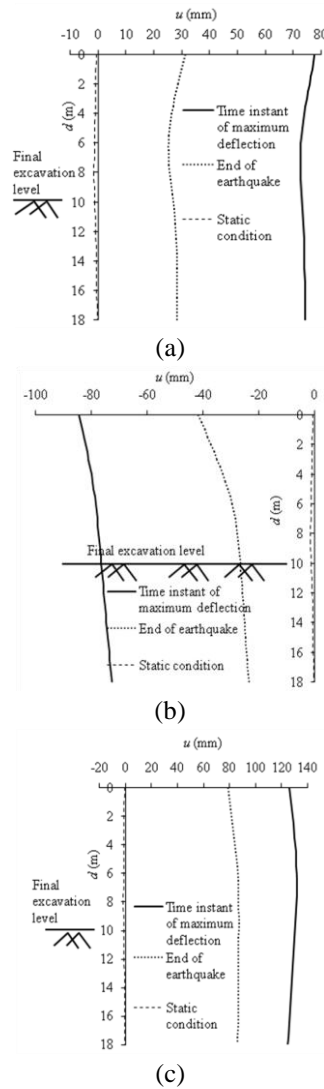
Fig. 11 Wall deflection profile of right wall when D_e=10 m for (a) Loma Prieta earthquake (b) Tolmezzo earthquake and (c) Northridge earthquake

25×10^5 kN/m/m, the wall deflection remains almost constant. Similarly, for D_b=8 m, k_{strut}=5×10^5 kN/m/m and t_{wall}/D_e is increased from 0.06 to 0.07, no significant change in the wall deflection is observed. Thus, it can be said that under seismic condition to get the best possible results in terms of lateral wall deflection, the depth of embedment can be chosen as 80% to 100% of the depth of excavation.

3.2.4 Effect of earthquake on maximum vertical ground displacement

The ground surface displacement in the final stage of excavation under static condition (v_{stat}) and at the end of earthquake (v_{seis}) is shown in Table 5. The values for ground displacement at the end of earthquake are calculated within range of 20 m from the face of retaining wall. It may be found
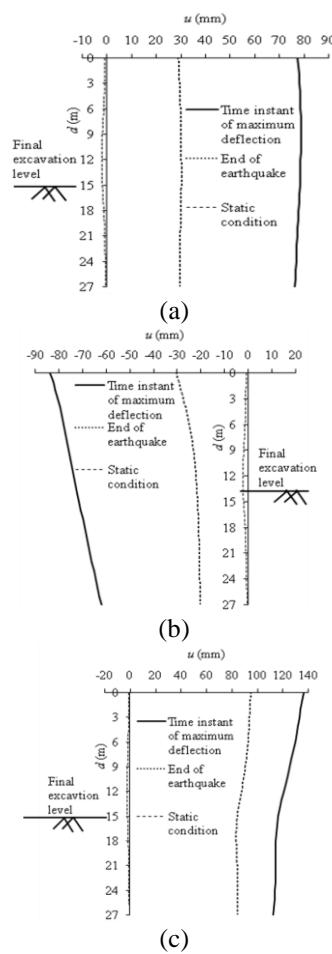
Fig. 12 Wall deflection profile of right wall when D_e=15 m for (a) Loma Prieta earthquake (b) Tolmezzo earthquake and (c) Northridge earthquake

Table 5 Variation of ground surface displacement for different values of D_e and earthquakes

D_e (m)	Side of excavation	Static (v_{stat})	Maximum ground surface displacement (mm)					
			Earthquake					
			Loma Prieta (PGA=0.28 g)		Tolmezzo (PGA=0.35 g)		Northridge (PGA=0.54 g)	
			End of EQ. (v_{seis})	v_{seis}/v_{stat}	End of EQ. (v_{seis})	v_{seis}/v_{stat}	End of EQ. (v_{seis})	v_{seis}/v_{stat}
10	Left	+2.1	+4.0	1.9	-17.5	8.3	-12.9	6.1
	Right	+2.1	+2.5	1.2	-19.3	9.2	-8.2	3.9
15	Left	+3.4	+6.0	1.7	-8.6	2.5	+2.2	0.7
	Right	+3.4	+6.8	2.0	-5.9	1.7	+5.3	1.6
20	Left	+4.3	+9.9	2.3	-5.0	1.2	+7.6	1.8
	Right	+4.3	+11.7	2.7	+6.6	1.5	+5.7	1.3

'-' indicates settlement and '+' indicates heaving
The value of v_{seis}/v_{stat} is calculated on the basis of absolute magnitude of the above values of v_{seis}
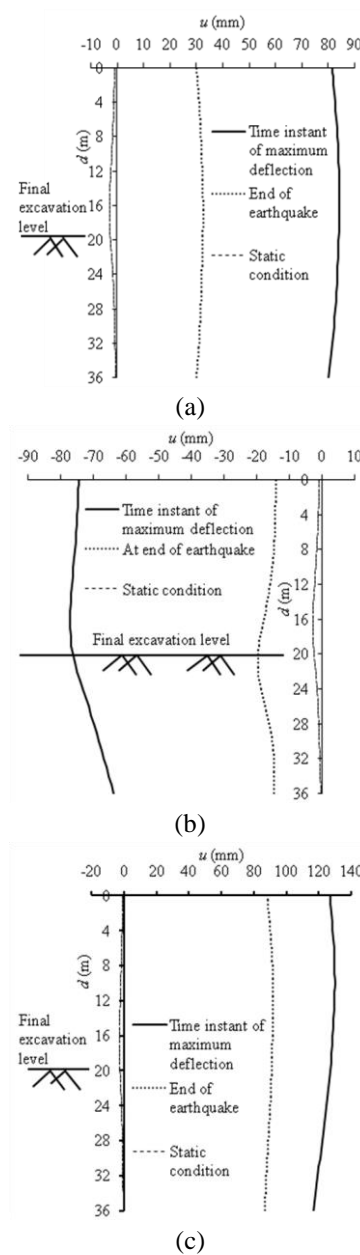
(a)

(b)

(c)

Fig. 13 Wall deflection profile of right wall when D_e=20 m for (a) Loma Prieta earthquake (b) Tolmezzo earthquake and (c) Northridge earthquake

from the table that there is large difference between the ground displacement between static and seismic conditions. If R_v is defined as the ratio between v_{seis} and v_{stat}, then it is observed that when the depth of excavation is 10m, the values of R_v are 1.9, 9.2, 6.1 for Loma Prieta, Tolmezzo and Northridge earthquakes, respectively. However, when D_e=15 m, the values of R_v are 2.0, 2.5, 1.6 for Loma Prieta, Tolmezzo and Northridge earthquakes, respectively. Similarly, when the depth of

excavation is 20m, the values of R_v are 2.7, 1.5, 1.8 for Loma Prieta, Tolmezzo and Northridge earthquakes, respectively. Thus, the maximum ground displacement at the end of earthquake is approximately 1-9 times higher than that under static condition.

It can be found from Table 4 that if the depth of embedment is increased from 8 m to 10 m, the ground surface displacement under seismic condition (v_{seis}) decreases by 44%. However, if D_b is increased from 10 m to 12 m, there is increment of 20% in ground displacement. This happens because of the depth of embedment which plays an important role in reducing ground surface displacement under static condition as well as seismic condition. However, under seismic condition, the seismic wave travels upward through the soil and reaches the ground surface at different amplitudes. Thus, the ground surface displacement may increase or decrease, if the depth of embedment is decreased. If k_{strut} is increased from 5×10^5 kN/m/m to 25×10^5 kN/m/m, the value of v_{seis} is increased by 24%. However, if D_b=8 m, k_{strut}=5×10^5 kN/m/m and t_{wall}/D_e is increased from 0.06 to 0.07, the ground displacement is decreased by 6%. Thus, it may be said that to get the best possible results in terms of lateral wall deflection under seismic condition, the depth of embedment may be chosen around 100% of the depth of excavation. However, higher wall thickness may be considered to get slightly lower surface displacement.

4. Conclusions

On the basis of the geometry of the underground retaining structure, type of soil and the earthquakes considered in the present study, it can be concluded that the strut force under seismic condition is approximately 2-3 times higher than that under static condition. It is further observed that the wall deflection is most sensitive to earthquake effect as compared to the other design parameters. To get the best possible results under seismic condition, the embedment depth of the wall may be chosen as around 100% of the depth of final excavation level. The stiffness of the strut and thickness of the wall may be chosen as 5×10^5 kN/m/m and 6% of depth of excavation, respectively to get the best possible performance in terms of strut force, wall moment and lateral wall deflection. However, under seismic condition to achieve lower ground displacement, thicker wall (t_{wall}=0.07D_e or more) can be used, but in such case higher strut force and wall moment will develop. Some of the limitations in the present study include the use of elastic-perfectly plastic Mohr-Coulomb model, which approximates the real behavior of soil. However, this has been used because, of its simplicity and wide application to model the soil. The analysis has been done for three earthquakes of different intensities and similar trend of results are obtained for all the selected earthquakes. The range of PGA is in between 0.28 g and 0.54 g. This range is wide and high enough to cover most of the known earthquakes. Thus, the trends those are obtained in the present study can be valid for other earthquakes also. The recommendations can also be valid for other earthquakes. However, values of maximum bending moment, wall deflection, strut force, ground deformation may vary for different earthquakes.

Acknowledgments

References

Abuhajar, O., Naggar, H.E. and Newson, T. (2011), "Effects of underground structures on amplification of seismic motion for sand with varying density", *Pan-Am CGS Geotechnical Conference*, October 2-6, 2011, Toronto, Ontario, Canada.

Atik, L.A. and Sitar, N. (2010), "Seismic earth pressures on cantilever retaining structures", *J. Geotech. Geoenviron. Eng.*, **136**(10), 1324-1333.

Aversa, S., Maiorano, R.M.S. and Tamagnini, C. (2007), "Influence of damping and soil model on the computed seismic response of flexible retaining structures", *In 14th European Conference on Soil Mechanics and Geotechnical Engineering.*

Bose, S.K. and Som, N.N. (1998), "Parametric study of a braced cut by Finite Element method", *Comput. Geotech.*, **22**(2), 91-107.

Callisto, L., Soccodato, F.B. and Conti, R. (2008), "Analysis of the seismic behavior of propped retaining structures", *Proceedings of Geotechnical Earthquake Engineering and Soil Dynamivs IV conference*, *GSP 181*, Sacramento, USA.

Callisto, L. and Soccodato, F.M. (2010), "Seismic design of flexible cantilever retaining walls", *J. Geotech. Geoenviron. Eng.*, **136**(2), 344-354.

Caltabiano, S., Cascone, E. and Maugeri, M. (2000), "Seismic stability of retaining walls with surcharge", *Soil Dyn. Earthq. Eng.*, **20**(8), 469-476.

Carrubba, P. and Colonna, P. (2000), "A comparison of numerical methods for multi-tied walls", *Comput. Geotech.*, **27**(2), 117-140.

Chowdhury, S.S., Deb, K. and Sengupta, A. (2013), "Estimation of design parameters for braced excavation: A numerical study", *Int. J. Geomech.*, **13**(3), 234-247.

Conti, R., Viggiani, G.M.B. and Madabhusi, S.P.G. (2010), *Physical modeling of flexible retaining walls under seismic actions*, *Physical Modelling in Geotechnics*, Eds. Springman, Laue and Seward, Taylor & Francis Group, London.

Costa, P.A., Borges, J.L. and Fernandes, M.M. (2007), "Analysis of a braced excavation in soft soils considering the consolidation effect", *J. Geotech. Geologic. Eng.*, **25**(6), 617-629.

Day, R.A. and Potts. D.M. (1993), "Modeling sheet pile retaining walls", *Comput. Geotech.*, **15**(3), 125-143.

Gazetas, G., Psarropoulos, P.N., Anastasopoulos, I. and Gerolymos, N. (2004), "Seismic behavior of flexible retaining systems subjected to short-duration moderately strong excitation", *Soil Dyn. Earthq. Eng.*, **24**(7), 537-550.

Georgiadis, M. and Anagnostopoulos, C. (1999), "Displacement of structures adjacent to cantilever sheet pile walls", *Soil. Found.*, **39**(2), 99-104.

Finno, R.J., Harahap, I.S. and Sabatini, P.J.M. (1991), "Analysis of braced excavations with coupled finite element formulations", *Comput. Geotech.*, **12**(2), 91-114.

Finno, R.J. and Harahap, I.S. (1991), "Finite Element Analysis of HDR-4 excavation", *J. Geotech. Eng. Div.*, **117**(10), 1590-1609.

His, J.P. and Small, J.C. (1993), "Application of a fully coupled method to the analysis of an excavation", *Soil. Found.*, **33**(4), 36-48.

Hsieh, P.G. and Ou, C.Y. (1998), "Shape of ground surface settlement profiles caused by excavation", *Can. Geotech. J.*, **35**(6), 1004-1117.

Hsiung, B.C.B. (2009), "A case study on the behavior of a deep excavation in sand", *Comput. Geotech.*, **36**(4), 665-675.

Itasca (2005), *FLAC Fast Lagrangian Analysis of Continua*, v.5.0, User's Manual.

Jr. Richards, R., Huang, M. and Fishman, K.L. (1999), "Seismic earth pressure on retaining structures", *J. Geotech. Geoenviron. Eng.*, **125**(9), 771-778.

Karlsrud, K. and Andresen, L. (2005), "Loads on braced excavation in soft clay", *Int. J. Geomech.*, **5**(2), 107-113.

Kung, G.T.C., Juang, C.H., Hsiao, E.C.L. and Hashash, Y.M.A. (2007), "Simplified model for wall

deflection and ground-surface settlement caused by braced excavation in clays", *J. Geotech. Geoenviron. Eng.*, **133**(6), 731-747.

Kung, G.T.C. (2009), "Comparison of excavation-induced wall deflection using top-down and bottom-up construction methods in Taipei silty clay", *Comput. Geotech.*, **36**(3), 373-385.

Ling, H.I., Mohri, Y., Leshchinsky, D., Burke, C., Matsushima, K. and Liu, H. (2005), "Large scale shaking table tests on modular block-reinforced soil retaining walls", *J. Geotech. Geoenviron. Eng.*, **131**(4), 465-476.

Ling, H.I., Liu, H. and Mohri, Y. (2005), "Parametric studies on the behavior of reinforced soil retaining walls under earthquake loading", *J. Eng. Mech.*, **131**(10), 1056-1065.

Ling, H.I., Leshchinsky, D., Wang, J.P., Mohri, Y. and Rosen, A. (2009), "Seismic response of geocell retaining walls: Experimental studies", *J. Geotech. Geoenviron. Eng.*, **135**(4), 515-524.

Liu, G.B., Ng, C.W.W. and Wang, Z.W. (2005), "Observed performance of a deep multi-strutted excavation in Shanghai soft clays", *J. Geotech. Geoenviron. Eng.*, **131**(8), 1004-1013.

Long, M. (2001), "Database for retaining wall and ground movements due to deep excavations", *J. Geotech. Geoenviron. Eng.*, **127**(3), 203-224.

Lysmer, J. and Kuhlemeyer, R.L. (1969), "Finite dynamic model for infinite media", *J. Eng. Mech.*, **95**(EM4), 859-877.

Madabhushi, S.P.G. and Zeng, X. (1998), "Seismic response of gravity quay walls. I: Numerical modeling", *J. Geotech. Geoenviron. Eng.*, **124**(5), 418-427.

Madabhushi, S.P.G. and Zeng, X. (2008), "Simulating seismic response of cantilever retaining walls", *J. Geotech. Geoenviron. Eng.*, **133**(5), 539-549.

Moormann, C. (2004), "Analysis of wall and ground movements due to deep excavations in soft soil based on a new worldwide database", *Soils Found.*, **44**(1), 87-98.

Nakai, T., Kawano, H., Murata, K., Banno, M. and Hashimoto, T. (1999), "Model test and numerical simulation of braced excavation in sandy ground: Influences of construction history, wall friction, wall stiffness, strut position and strut stiffness", *Soils Found.*, **39**(3), 1-12.

Neelakantan, G., Budhu, M. and Jr. Richards, R. (1992), "Balanced seismic design of anchored retaining walls", *J. Geotech. Eng. Div.*, **118**(6), 873-888.

Ng, C.W.W., Simpson, B., Lings, M.L. and Nash, D.F.T. (1998), "Numerical analysis of a multipropped retaining wall in stiff clay", *Can. Geotech. J.*, **35**(1), 115-130.

Ou, C.Y. and Hsieh, P.G. (2011), "A simplified method for predicting ground settlement profiles induced by excavation in soft clay", *Comput. Geotech.*, **38**(8), 987-997.

Psarropoulos, P.N., Klonaris, G. and Gazetas, G. (2005), "Seismic earth pressures on rigid and flexible retaining walls", *Soil Dyn. Earthq. Eng.*, **25**(10), 795-809.

Siller, T.J. and Frawley, D.D. (1992), "Seismic response of multianchored retaining walls", *J. Geotech. Geoenviron. Eng.*, **118**(11), 1787-1803.

Takemura, J., Kondoh, M., Esaki, T., Kouda, M. and Kusakabe, O. (1999), "Centrifuge model tests on double propped wall excavation in soft clay", *Soil. Found.*, **39**(3), 75-87.

Tanaka, H. (1999), "Behavior of a braced excavation in soft clay and the undrained shear strength for passive earth pressure", *Soils Found.*, **34**(1), 53-64.

Tefera, T.H., Nordal, S., Grande, L., Sandven, R. and Emdal, A. (2006), "Ground settlement and wall deformation from a large scale model test on as single strutted sheet pile wall in sand", *Int. J. Physic. Model. Geotech.*, **6**(2), 1-13.

Tufenkjian, M.R. and Vucetic, M. (2000), "Dynamic failure mechanism of soil-nailed excavation models in centrifuge", *J. Geotech. Geoenviron. Eng.*, **126**(3), 227-235.

Wang, Z.W., Ng, C.W.W. and Liu, G.B. (2005), "Characteristics of wall deflections and ground surface settlements in Shanghai", *Can. Geotech. J.*, **42**(5), 1243-1254.

Wang, J.H., Xu, Z.H. and Wang, W.D. (2010), "Wall and ground movements due to deep excavations in Shanghai soft soils", *J. Geotech. Geoenviron. Eng.*, **136**(7), 985-994.

Wartman, J., Rondinel-Oviedo, E.A. and Rodriguez-Marek, A. (2006), "Performance and analyses of Mechanically Stabilized earth walls in the Tecoman, Mexico Earthquake", *J. Perform. Constr. Fac.*,

20(3), 287-299.

Watanabe, K., Munaf, Y., Koseki, J., Tateyama, M. and Kojima, K. (2003), "Behaviors of several types of model retaining walls subjected to irregular excitation", *Soils Found.*, **43**(5), 13-27.

Yogendrakumar, M. Bathurst, R.J. and Finn, W.D.L. (1992), "Dynamic response analysis of reinforced soil retaining wall", *J. Geotech. Geoenviron. Eng.*, **118**(8), 1158-1167.

Yoo, C. and Lee, D. (2008), "Deep excavation-induced ground surface movement characteristics-A numerical investigation", *Comput. Geotech.*, **35**(2), 231-252.

Zdravkovic, L. Potts, D.M. and St. John, H.D. (2005), "Modeling of a 3D excavation in finite element analysis", *Geotechnique*, **55**(7), 497-513.

Zeng, X. (1998), "Seismic response of gravity quay walls. I: Centrifuge modeling", *J. Geotech. Geoenviron. Eng.*, **124**(5), 406-417.

IT

Notations

The following symbols are used in this paper:

A_{wall}=cross-sectional area of the wall

A_{strut}=cross-sectional area of the wall

a=parameter for sigmoidal model in FLAC

B=width of excavation

b=parameter for sigmoidal model in FLAC

C_S=shear wave speed

D_e=maximum excavation depth (final stage)

D_b=embedded depth (final stage)

f_{max}=maximum frequency

E_{strut}=Young's modulus of the strut

E_{wall}=Young's modulus of the wall

F=maximum axial force in the strut

F_{stat}=axial force in the strut under static condition

F_{seis}=axial force (maximum value) in the strut under seismic condition

$R_F=F_{seis}/F_{stat}$

g=acceleration due to gravity

G_0=small strain shear modulus of soil

G_{st}=shear modulus of soil used in static simulation

G_d=shear modulus of soil used in dynamic simulation

G_s=secant shear modulus of soil

I_{wall}=moment of inertia of the wall

K_G=stiffness multiplier

K_{st}=bulk modulus of soil used in static simulation

K_d=bulk modulus of soil used in dynamic simulation

K_o=coefficient of lateral earth pressure at rest

K_n=interface normal stiffness between wall and soil

K_s=interface shear stiffness between wall and soil

k_{strut}=strut or support member stiffness

k_{wall}=wall stiffness
l=length of strut or support member
M=maximum bending moment in the wall
M_{stat}=moment in the wall under static condition
M_{seis}=moment (maximum value) in the wall under seismic condition
$R_M=M_{seis}/M_{stat}$
M_s=normalized secant shear modulus of soil
p'=mean effective stress
p_{ref}=reference pressure
s=horizontal spacing of strut or support members
t=time
t_{wall}=thickness of the wall
u=maximum horizontal wall deflection
u_{stat}=deflection of wall under static condition
u_{seis}=deflection (maximum value) of wall under seismic condition
$R_u=u_{seis}/u_{stat}$
t_s=slab thickness
v=maximum vertical ground displacement
v_{stat}=displacement of the ground surface under static condition
v_{seis}=displacement (maximum value) of the ground surface under seismic condition
$R_v=v_{seis}/v_{stat}$
x_0=parameter for sigmoidal model in FLAC
y_0=parameter for sigmoidal model in FLAC
Δz_{min}=smallest width of an adjoining element in the normal direction to the interface
δ=wall friction angle
ρ=density of soil
Δl=spatial element size
γ=shear strain in soil
λ=the wavelength associated with highest frequency component that contains appreciable energy
ϕ=friction angle
μ=Poisson's ratio of soil
μ_{wall}=Poisson's ratio of wall
τ=shear stress in soil